Stochastic Analysis and Applications

ISSN: 0736-2994 (Print) 1532-9356 (Online) Journal homepage: https://www.tandfonline.com/loi/lsaa20

Computational scheme for solving nonlinear fractional stochastic differential equations with delay

B. P. Moghaddam, A. Mendes Lopes, J. A. Tenreiro Machado & Z. S. Mostaghim

To cite this article: B. P. Moghaddam, A. Mendes Lopes, J. A. Tenreiro Machado & Z. S. Mostaghim (2019) Computational scheme for solving nonlinear fractional stochastic differential equations with delay, Stochastic Analysis and Applications, 37:6, 893-908, DOI: 10.1080/07362994.2019.1621182

To link to this article: https://doi.org/10.1080/07362994.2019.1621182

STOCHASTIC ANALYSIS AND APPLICATIONS
2019, VOL. 37, NO. 6, 893–908
https://doi.org/10.1080/07362994.2019.1621182

Taylor & Francis
Taylor & Francis Group

Computational scheme for solving nonlinear fractional stochastic differential equations with delay

B. P. Moghaddam[a,b], A. Mendes Lopes[b], J. A. Tenreiro Machado[c], and Z. S. Mostaghim[a]

[a]Department of Mathematics, Lahijan Branch, Islamic Azad University, Lahijan, Iran; [b]UISPA-LAETA/INEGI, Faculty of Engineering, University of Porto, Porto, Portugal; [c]Department of Electrical Engineering, Institute of Engineering, Porto, Portugal

ABSTRACT

This paper studies the numerical solution of fractional stochastic delay differential equations driven by Brownian motion. The proposed algorithm is based on linear B-spline interpolation. The convergence and the numerical performance of the method are analyzed. The technique is adopted for determining the statistical indicators of stochastic responses of fractional Langevin and Mackey-Glass models with stochastic excitations.

ARTICLE HISTORY
Received 7 June 2018
Accepted 12 February 2019

KEYWORDS
Fractional calculus; stochastic calculus; delay differential equation; numerical method; linear B-spline interpolation

2010 MSC
26A33; 34K37; 34K50; 60H35

1. Introduction

Many experiments and observations in real phenomena reveal stochastic effects. One well-known example is the Brownian motion exhibited by pollen when submerged in a fluid and subject to collisions with the fluid molecules [1]. Stochastic behavior can be also observed in population dynamics [2], epidemics [3, 4], motions of ions in crystals [5], thermal noise [6], stock indices [7], option pricing [8, 9], and optimal pricing in economics [10]. The study of stochasticity was first investigated by Einstein [11], Smoluchowski [12] and Langevin [13], and later extended by Ornstein and Uhlenbeck [14]. Concurrently with the development of the concepts and applications of stochastic calculus, we witness the expanding application of fractional calculus, due to the nonlocal properties of fractional operators [15–22]. The fractional-order operators have been employed for designing high-performance controllers for dynamical systems [23, 24], modeling viscoelastic materials [25, 26], realistic impact phenomena [27], etc.

Many problems in physics, chemistry, biology, finance, and engineering have been modeled as fractional stochastic differential or integral equations [28–31]. Numerical methods for simulating models based on fractional and stochastic calculus are important for understanding and unveiling the properties of many phenomena. In the same line of thought were

CONTACT B. P. Moghaddam parsa@liau.ac.ir Department of Mathematics, Lahijan Branch, Islamic Azad University, Lahijan, P.O. Box:1616, Iran.
Color versions of one or more of the figures in the article can be found online at www.tandfonline.com/lsaa.

developed numerical approaches for some classes of stochastic differential equations (SDEs) driven by Brownian motion process, namely methods such as Monte Carlo, for stochastic evolution equations with Riesz-fractional spatial derivative [32], meshfree, based on radial basis functions, and Gauss-Legendre quadrature rule [33], and shifted Legendre spectral collocation, to solve fractional stochastic integro-differential equations [34]. Moreover, explicit discrete schemes based on the Simpson's quadrature formula, to simulate the response of fractional dynamic systems in noisy environments [35]. There are various approaches for evaluating the approximate solution of SDE driven by a fractional Brownian motion process, and we can mention methods such as mean-square dissipative [36], cardinal wavelets [37], collocation via the hat functions [38, 39], and Euler polynomials [40].

The existence and uniqueness of solutions of fractional stochastic delay differential equation (FSDDE) has already been tackled [41–45], but to the best authors' knowledge there is no research on numerical methods for their solution.

Hereafter we consider the FSDDE as

$$\begin{cases} {}_0^C\mathscr{D}_t^{\varrho} u(t) = f\big(t, u(t), u(t-\delta)\big) + g(t, u(t))\dfrac{d\omega(t)}{dt}, & t \in \big(0, T_f\big] \\ u(t) = \psi(t), & t \in [-\delta, 0] \end{cases}, \tag{1}$$

where $\frac{1}{2} < \varrho < 1, f : [0, T_f] \times \mathbb{R} \times \mathbb{R} \to \mathbb{R}$ and $g : [0, T_f] \times \mathbb{R} \to \mathbb{R}$ are measurable functions, δ represents the delay time, $\psi(t)$ is the history function defined on the interval $t \in [-\delta, 0]$, and $\omega(t)$ denotes a Wiener process. The solutions of stochastic delay differential equations do not follow the Markov property, and their representations are more complex than those of stochastic differential equations. In addition, we cannot obtain the exact analytical solution of a given FSDDE (1) and, therefore, in order to predict the behavior of sample trajectories of solutions, we need to investigate the confidence interval (CI) of the exact solutions by means of numerical approximations [46].

This work is organized as follows. Section 2 describes the main definitions that will be used through this study. Section 3 presents an explicit method based on linear B-spline interpolation for discretizing a class of FSDDEs driven by Brownian motion. Section 4 discusses the convergence of the proposed algorithm for approximating the solution of (1). Section 5 examines the performance of the novel approach for two models, namely the Langevin and the Mackey-Glass models. Finally, section 6 draws the conclusions.

2. Preliminaries

In this paper, we assume that $\mathbb{L}^2(\Omega, \mathcal{F}_t, \mathbb{P})$ is a probability space of all $\mathcal{F}_t$-measurable, mean square integrable functions $u : \Omega \to \mathbb{R}$ with

$$||u||_{ms} := \mathbb{E}\big(||u||^2\big)^{\frac{1}{2}},$$

where $||\cdot||$ is the standard Euclidean norm. The probability space $\mathbb{L}^2(\Omega, \mathcal{F}_t, \mathbb{P})$ is generated by a one-dimensional standard Wiener process $\omega(t) : \mathbb{R}^+ \to \mathbb{R}$, with the following properties [47]

1. $\omega(0) = 0$;
2. $\omega(t)$ has independent increment;
3. For every $t > s \geq 0, \omega(t) - \omega(s)$ follows a normal distribution with zero-mean and $(t-s)$-variance.

Definition 1 ([48]). A Gaussian white noise, $\eta(t)$, is the derivative of the Wiener process, as follows

$$\eta(t) = \sigma \frac{d\omega(t)}{dt}, \tag{2}$$

with zero expectation, $E(\eta(t)) = 0$, and finite variance σ^2, that is, $Var(\eta(t)) = \sigma^2$.

Definition 2 ([49]). The stochastic integral $\int_0^t r(\zeta)d\omega(\zeta)$ with Itô's isometry, is defined as

$$\mathbb{E}\left[\left(\int_0^t r(\zeta)d\omega(\zeta)\right)^2\right] = \mathbb{E}\left[\int_0^t r^2(\zeta)d\zeta\right], \tag{3}$$

where $r : \mathbb{R} \times \mathbb{R} \to \mathbb{R}$*is a measurable function.*

Definition 3 ([50]). The left-sided Riemann-Liouville fractional integral of order ϱ, for a function u(t) is defined as

$${}_0\mathcal{J}_t^{\varrho} u(t) = \frac{1}{\Gamma(\varrho)} \int_0^t u(\zeta)(t-\zeta)^{\varrho-1} d\zeta, \tag{4}$$

where t, ϱ, and $\zeta \in \mathbb{R}^+$ and $\Gamma(\cdot)$ denotes the Gamma function.

Definition 4 ([50]). The left-sided Caputo fractional-order derivative of order $\varrho \in \mathbb{R}^+$, is defined as

$${}_0^C\mathcal{D}_t^{\varrho} u(t) = \frac{1}{\Gamma(1-\varrho)} \int_0^t \frac{u'(\zeta)}{(t-\zeta)^{\varrho}} d\zeta, \quad 0 < \varrho \leq 1. \tag{5}$$

3. Proposed numerical algorithm

In this section, we propose a new numerical technique for solving the FSDDE (1) under the following hypothesis:

(H_1) The function $f(t, \cdot, \cdot)$ satisfies the Lipschitz condition in its second and third variables

$$\| f(t, u_1, \hat{u}_1) - f(t, u_2, \hat{u}_2) \| \leq L \| u_1 - u_2 \| + R \| \hat{u}_1 - \hat{u}_2 \|, \tag{6}$$

and the function $g(t, \cdot)$ satisfies the Lipschitz condition in its second variable:

$$\| g(t, u_1) - g(t, u_2) \| \leq \hat{L} \| u_1 - u_2 \|, \tag{7}$$

where L, R, and $\hat{L}$ are positive real constants.

(H_2) The function $f(\cdot, \cdot, 0)$ is $\mathbb{L}^2$ integrable, i.e.

$$\int_0^{\infty} ||f(\zeta, \zeta - \delta, 0)|| d\zeta < \infty,$$

and $g(\cdot, 0)$ is essentially bounded, i.e.

$$||g(\cdot,0)||_\infty := \operatorname{ess}\sup_{s\in[0,\infty]} ||g(s,0)|| < \infty.$$

For the initial condition $u(0) = u_0 \in \mathbb{L}^2(\Omega, \mathcal{F}_t, \mathbb{P})$, the FSDDE (1) can be written as

$$u(t) = u_0 + {}_0\mathcal{J}_t^\varrho f\big(t, u(t), u(t-\delta)\big) + {}_0\mathcal{J}_t^\varrho \left(g(t,u(t))\frac{d\omega(t)}{dt}\right). \tag{8}$$

We assume that $t_j = jh, j = -r, -r+1, ..., -1, 0, 1, ..., n,$ are regular spaced mesh points in the interval $[0, T_f]$, such that $r = \frac{\delta}{h}, n = \frac{T_f}{h}$ and $r, n \in \mathbb{Z}$.

Proposition 3.1 ([51]). *Let $y(t)$ be a function in $C^2[0, T_f]$ and $\varrho > 0$. Then*

$${}_0\mathcal{J}_{t_n}^\varrho y(t) = \frac{h^\varrho}{\Gamma(\varrho+2)}\sum_{j=0}^{n}\sigma_{j,n}y(t_j) + \mathcal{O}(h^{2+\varrho}), \tag{9}$$

where

$$\sigma_{j,n} = \begin{cases} (n-1)^{\varrho+1} - (n-\varrho-1)(n)^\varrho, & j = 0 \\ (n-j+1)^{\varrho+1} - 2(n-j)^{\varrho+1} + (n-j-1)^{\varrho+1}, & 1 \le j \le n-1, \\ 1, & j = n \end{cases} \tag{10}$$

and the truncated error of the (9) satisfies

$$||{}_0\mathcal{J}_{t_n}^\varrho\big[y(t)\big] - \Big({}_0\mathcal{J}_{t_n}^\varrho\big[y(t)\big]\Big)_{approx}|| \le K_1 h^{2+\varrho}, \tag{11}$$

where $K_1 = \frac{n^\varrho M h^{2+\varrho}}{\Gamma(\varrho+1)}$ and $||y''(t)|| \le M$.

Lemma 3.1. *The coefficients $\sigma_{j,n}$ in (10), $0 < \varrho < 1$, satisfy the properties:*

i. *The coefficients $\sigma_{j,n}, j = 0, 1, 2, ..., n-1$, are positive;*
ii. *The sum $\sum_{j=0}^{n-1}\sigma_{j,n}$ is convergent and positive.*

Proof. For $1 \le j \le n-1$, the coefficients $\sigma_{j,n}$ are given by

$$\begin{aligned}\sigma_{j,n} &= (n-j+1)^{\varrho+1} - 2(n-j)^{\varrho+1} + (n-j-1)^{\varrho+1} \\ &= \big((n-j+1)^{\varrho+1} - (n-j)^{\varrho+1}\big) - \big((n-j)^{\varrho+1} - (n-j-1)^{\varrho+1}\big).\end{aligned}$$

Therefore, the conclusion of the mean value theorem to the continuous function $g(x) = x^{\varrho+1}$, states that there exist points $\theta_1 \in (n-j, n-j+1)$ and $\theta_2 \in (n-j-1, n-j)$, such that

$$\begin{aligned}a_{k,n}^{(\alpha)} &= (\varrho+1)\theta_1^\varrho - (\varrho+1)\theta_2^\varrho \\ &= (\varrho+1)\big(\theta_1^\varrho - \theta_2^\varrho\big).\end{aligned} \tag{12}$$

Obviously, for $0 < \varrho < 1$ and $\theta_1 > \theta_2$, we obtain $\theta_1^\varrho - \theta_2^\varrho > 0$ and, therefore, from (12), we get $\sigma_{j,n} > 0$. Furthermore, we have

$$\sum_{k=0}^{n-1}\sigma_{j,n} = (\varrho+1)n^\varrho - 1 > 0,$$

that completes the proof.

Proposition 3.2. *Let $y(t)$ be a function in $\mathbb{L}^2(\Omega, \mathcal{F}_t, \mathbb{P})$ and for every subinterval $t \in [t_j, t_{j+1}] \subseteq [0, T_f), y(t) \in C^2[t_j, t_{j+1}]$ and $||y''(t)|| \leq M,\ j = 0, 1, ..., n-1$. Then*

$$ {}_0\mathcal{J}^{\varrho}_{t_n}\left[y(t)\eta(t)\right] = \frac{h^{\varrho}}{\Gamma(\varrho+2)}\sum_{j=0}^{n}\sigma_{j,n}y(t_j)\eta(t_j) + \mathcal{O}(h^{\varrho+\frac{3}{2}}), \tag{13} $$

where $\eta(t)$ Gaussian white noise, $\varrho > \frac{1}{2}$ and the truncated error of the (13) satisfies

$$ ||{}_0\mathcal{J}^{\varrho}_{t_n}\left[y(t)\eta(t)\right] - \left({}_0\mathcal{J}^{\varrho}_{t_n}\left[y(t)\eta(t)\right]\right)_{approx}||_{ms} \leq K_2 h^{\varrho+\frac{3}{2}}, \tag{14} $$

where $K_2 = \frac{n^{\varrho-\frac{1}{2}}M}{2\sqrt{(2\varrho-1)}\Gamma(\varrho)}$, and $\sigma_{j,n}$ is defined as (10).

Proof. The B-linear spline $s_j(t)$, as an approximation of $y_j(t)$ in the subinterval $[t_j, t_{j+1}] \subseteq [0, t_n) = [0, T_f),\ j = 0, 1, ..., n-1$, is given by:

$$ y_j(t) \approx s_j(t) = \frac{t-t_{j+1}}{t_j - t_{j+1}}y(t_j) + \frac{t-t_j}{t_{j+1}-t_j}y(t_{j+1}), \tag{15} $$

and

$$ \mathscr{E}_j(t) = y_j(t) - s_j(t) = \frac{y''(\varphi_j)}{2!}(t-t_j)(t-t_{j+1}), $$

where φ_j is an arbitrary value belonging to (t_j, t_{j+1}).

Let $\mathscr{E}(t)$ be the error function in the interval $(0, t_n]$. Therefore

$$ \begin{aligned} \mathbb{E}\left[||{}_0\mathcal{J}^{\varrho}_{t_n}[y(t)\eta(t)] - ({}_0\mathcal{J}^{\varrho}_{t_n}[y(t)\eta(t)])_{approx}||^2\right] &= \mathbb{E}\left[||\frac{1}{\Gamma(\varrho)}\int_0^{t_n}(t_n-\zeta)^{\varrho-1}\mathscr{E}(\zeta)\eta(\zeta)d\zeta||^2\right] \\ &= \mathbb{E}\left[||\frac{1}{\Gamma(\varrho)}\int_0^{t_n}(t_n-\zeta)^{\varrho-1}\mathscr{E}(\zeta)d\omega(\zeta)||^2\right]. \end{aligned} $$

Using Itô's isometry property (Definition 2), we have

$$ \begin{aligned} &\mathbb{E}\left[||{}_0\mathcal{J}^{\varrho}_{t_n}[y(t)\eta(t)] - ({}_0\mathcal{J}^{\varrho}_{t_n}[y(t)\eta(t)])_{approx}||^2\right] \\ &= \mathbb{E}\left[\frac{1}{\Gamma^2(\varrho)}\int_0^{t_n}||(t_n-\zeta)^{\varrho-1}\mathscr{E}(\zeta)||^2 d\zeta\right] \\ &= \mathbb{E}\left[\frac{1}{\Gamma^2(\varrho)}\sum_{j=0}^{n-1}\int_{t_j}^{t_{j+1}}||(t_n-\zeta)^{\varrho-1}\mathscr{E}_j(\zeta)||^2 d\zeta\right] \\ &= \frac{1}{\Gamma^2(\varrho)}\mathbb{E}\left[\sum_{j=0}^{n-1}\int_{t_j}^{t_{j+1}}(t_n-\zeta)^{2\varrho-2}||\frac{y''(\varphi_j)}{2!}(\zeta-t_j)(\zeta-t_{j+1})||^2 d\zeta\right] \\ &\leq \frac{h^4}{\Gamma^2(\varrho)}\mathbb{E}\left[\frac{M^2}{4}\right]\sum_{j=0}^{n-1}\int_{t_j}^{t_{j+1}}(t_n-\zeta)^{2\varrho-2}d\zeta, \end{aligned} $$

where $||y''(\varphi_j)|| \leq M$.

Since $\varrho > \frac{1}{2}$, we get

$$\mathbb{E}\Big[||{}_0\mathcal{J}^{\varrho}_{t_n}[y(t)\eta(t)]-({}_0\mathcal{J}^{\varrho}_{t_n}[y(t)\eta(t)])_{approx}||^2\Big] \leq \frac{h^4M^2}{4\Gamma^2(\varrho)}\int_0^{t_n}(t_n-\zeta)^{2\varrho-2}d\zeta = \frac{h^4t_n^{2\varrho-1}M^2}{4(2\varrho-1)\Gamma^2(\varrho)} = \frac{n^{2\varrho-1}M^2h^{2\varrho+3}}{4(2\varrho-1)\Gamma^2(\varrho)}.$$

Hence,

$$||{}_0\mathcal{J}^{\varrho}_{t_n}\big[y(t)\eta(t)\big]-\Big({}_0\mathcal{J}^{\varrho}_{t_n}\big[y(t)\eta(t)\big]\Big)_{approx}||_{ms} \leq \left(\frac{n^{\varrho-\frac{1}{2}}M}{2\sqrt{(2\varrho-1)}\Gamma(\varrho)}\right)h^{\varrho+\frac{3}{2}} = \mathcal{O}(h^{\varrho+\frac{3}{2}}).$$

We can apply the Propositions 3.1 and 3.2 to discretize FSDDE (8) with a smaller step size h and we can write

$$\begin{aligned}&{}_0\mathcal{J}^{\varrho}_{t_n}f\big(t,u(t),u(t-\delta)\big)\\ &\approx \frac{h^{\varrho}}{\Gamma(\varrho+2)}\left(f(t_n,u_n,u_{n-r})+\sum_{j=0}^{n-1}\sigma_{j,n}f(t_j,u_j,u_{j-r})\right),\end{aligned} \tag{16}$$

and

$$\begin{aligned}{}_0\mathcal{J}^{\varrho}_{t_n}\left(g(t,u(t))\frac{d\omega(t)}{dt}\right) &= \frac{1}{\Gamma(\varrho)}\int_0^{t_n}(t-\zeta)^{\varrho-1}g(\zeta,u(\zeta))d\omega(\zeta)\\ &= \frac{1}{\Gamma(\varrho)}\int_0^{t_n}(t-\zeta)^{\varrho-1}g(\zeta,u(\zeta))\eta(\zeta)d\zeta\\ &\approx \frac{h^{\varrho}}{\Gamma(\varrho+2)}\left(g(t_n,u_n)\eta(t_n)+\sum_{j=0}^{n-1}\sigma_{j,n}g(t_j,u_j)\eta(t_j)\right).\end{aligned} \tag{17}$$

Therefore, from (16) and (17), we obtain

$$\begin{aligned}u_n = u_0 &+ \frac{h^{\varrho}}{\Gamma(\varrho+2)}\big(f(t_n,u_n,u_{n-r})+g(t_n,u_n)\eta(t_n)\\ &+\sum_{j=0}^{n-1}\sigma_{j,n}(f(t_j,u_j,u_{j-r})+g(t_j,u_j)\eta(t_j))\big),\end{aligned} \tag{18}$$

where $\sigma_{j,n}$ is defined as (10).

It is worth noting that in the case that $f(t,\cdot,\cdot)$ and $g(t,\cdot)$ are nonlinear with respect to their variables, to avoid solving a system of nonlinear equations, the nonlinear source terms are discretized in the following way:

$$||f(t_n,u_n,u_{n-r})-f(t_n,u_{n-1},u_{n-r})|| \leq L_2h = \mathcal{O}(h), \tag{19}$$

$$||g(t_n,u_n)-g(t_n,u_{n-1})|| \leq L_3h = \mathcal{O}(h), \tag{20}$$

where L_2 and L_3 are positive real Lipschitz constants for the functions f and g, respectively.

4. Convergence analysis

In this section, we analyze the convergence of the algorithm (18) in approximating the solution of the FSDDE (1).

Theorem 4.1. *Let $u(t) \in \mathbb{L}^2(\Omega, \mathcal{F}_t, \mathbb{P})$ be the exact solution of the FSDDE (1). Let us consider that $f(t,\cdot,\cdot)$ and $g(t,\cdot)$ satisfy H_1 and H_1 hypothesis. Furthermore, we assume that u_j, $j = 0, \ldots, n$, are the approximate solutions of the FSDDE (1), obtained from (18). Then*

$$||\mathscr{E}(t_n)||_{ms} \leq K^{(\varrho)} h^{\varrho+\frac{1}{2}} = \mathcal{O}\big(h^{\varrho+\frac{1}{2}}\big), \tag{21}$$

where $\mathscr{E}(t_n) = u(t_n) - u_n$ and $K^{(\varrho)}$ is a positive and real constant value independent of h.

Proof. From (8), for the time instant $t_n \in [0, T_f]$, we have

$$u(t_n) = u_0 + {}_0\mathcal{J}^{\varrho}_{t_n} f\big(t, u(t), u(t-\delta)\big) + {}_0\mathcal{J}^{\varrho}_{t_n}\left(g(t,u(t))\frac{d\omega(t)}{dt}\right). \tag{22}$$

We assume that $\mathscr{E}_0 = 0$. Subtracting (22) from (18) and using the elementary inequality

$$\left|\left|\sum_{k=1}^{s} x_k\right|\right|^2 \leq s\sum_{k=1}^{s}||x_k||^2, \tag{23}$$

and the Hölder inequality

$$||\mathscr{E}(t_n)||^2_{ms} = \mathbb{E}\Big[||\mathscr{E}(t_n)||^2\Big] \leq 2\mathbb{E}\Big[||\mathscr{E}_f(t_n)||^2\Big] + 2\mathbb{E}\Big[||\mathscr{E}_g(t_n)||^2\Big], \tag{24}$$

yields

$$\begin{aligned}
||\mathscr{E}(t_n)||^2_{ms} = \mathbb{E}\Bigg[\Bigg|\Bigg| &\frac{1}{\Gamma(\varrho)}\int_0^{t_n}(t_n-\zeta)^{\varrho-1} f(\zeta, u(\zeta), u(\zeta-\delta))d\zeta \\
&+ \frac{1}{\Gamma(\varrho)}\int_0^{t_n}(t_n-\zeta)^{\varrho-1} g(\zeta, u(\zeta))d\omega(\zeta) \\
&- \frac{h^{\varrho}}{\Gamma(\varrho+2)}\big(f(t_n, u_{n-1}, u_{n-r}) + g(t_n, u_{n-1})\eta(t_n)\big) \\
&+ \sum_{j=0}^{n-1}\sigma_{j,n}\big(f(t_j, u_j, u_{j-r}) + g(t_j, u_j)\eta(t_j)\big)\Bigg|\Bigg|^2\Bigg] \\
\leq 2\mathbb{E}\Bigg[\Bigg|\Bigg| &\frac{1}{\Gamma(\varrho)}\int_0^{t_n}(t_n-\zeta)^{\varrho-1} f(\zeta, u(\zeta), u(\zeta-\delta))d\zeta \\
&- \frac{h^{\varrho}}{\Gamma(\varrho+2)}\Big(f(t_n, u_{n-1}, u_{n-r}) + \sum_{j=0}^{n-1}\sigma_{j,n} f(t_j, u_j, u_{j-r})\Big)\Bigg|\Bigg|^2\Bigg] \\
&+ 2\mathbb{E}\Bigg[\Bigg|\Bigg| \frac{1}{\Gamma(\varrho)}\int_0^{t_n}(t_n-\zeta)^{\varrho-1} g(\zeta, u(\zeta))d\omega(\zeta) \\
&- \frac{h^{\varrho}}{\Gamma(\varrho+2)}\Big(g(t_n, u_{n-1})\eta(t_n) + \sum_{j=0}^{n-1}\sigma_{j,n} g(t_j, u_j)\eta(t_j)\Big)\Bigg|\Bigg|^2\Bigg].
\end{aligned}$$

The first term on the right-hand side of the upper inequality is

$$\mathbb{E}[||\mathscr{E}_f(t_n)||^2] := \mathbb{E}\left[\left\| \frac{1}{\Gamma(\varrho)}\int_0^{t_n} (t_n-\zeta)^{\varrho-1} f(\zeta, u(\zeta), u(\zeta-\delta))d\zeta \right.\right.$$
$$\left.\left. -\frac{h^\varrho}{\Gamma(\varrho+2)}(f(t_n, u_{n-1}, u_{n-r}) + \sum_{j=0}^{n-1}\sigma_{j,n} f(t_j, u_j, u_{j-r}))\right\|^2\right],$$

and using (23) and the Hölder inequality, one can show that

$$\mathbb{E}[||\mathscr{E}_f(t_n)||^2] \le 3\mathbb{E}\left[\left\| \frac{1}{\Gamma(\varrho)}\int_0^{t_n} (t_n-t)^{\varrho-1} f(t, u(t), u(t-\delta))dt \right.\right.$$
$$\left.\left. -\frac{h^\varrho}{\Gamma(\varrho+2)}\sum_{j=0}^{n}\sigma_{j,n} f(t_j, u(t_j), u(t_j-\delta)))\right\|^2\right]$$
$$+\frac{3nh^{2\varrho}}{\Gamma^2(\varrho+2)}\sum_{j=0}^{n-1}\sigma_{j,n}^2\mathbb{E}\left[\|f(t_j, u(t_j), u(t_j-\delta)) - f(t_j, u_j, u_{j-r})\|^2\right]$$
$$+\frac{3h^{2\varrho}}{\Gamma^2(\varrho+2)}\mathbb{E}\left[\|f(t_n, u(t_n), u(t_n-\delta)) - f(t_n, u_{n-1}, u_{n-r})\|^2\right].$$

By means of Lipschitz conditions and after some simplications, we obtain

$$\mathbb{E}\left[||\mathscr{E}_f(t_n)||^2\right] \le 3\left(\frac{n^{2+\varrho}Mh^{2+\varrho}}{\Gamma(\varrho+1)}\right)^2 + \frac{3nh^{2\varrho}}{\Gamma^2(\varrho+2)}\sum_{j=0}^{n-1}\sigma_{j,n}^2(L^2+R^2)\left(\frac{M^2h^4}{2}\right) + \frac{3h^{2\varrho}L_2^2}{\Gamma^2(\varrho+2)}h^2.$$

From Lemma 3.1, we have

$$\sum_{j=0}^{n-1}\sigma_{j,n}^2 \le n\left(\sum_{j=0}^{n-1}\sigma_{j,n}\right)^2 \le n\big((\varrho+1)n^\varrho-1\big)^2 = L_1. \tag{25}$$

Therefore

$$\mathbb{E}[||\mathscr{E}_f(t_n)||^2] \le 3\left(\left(\frac{n^{2+\varrho}M}{\Gamma(\varrho+1)}\right)^2 + \frac{n}{2\Gamma^2(\varrho+2)}L_1\left(L^2+R^2)M^2 + \frac{L_2^2}{\Gamma^2(\varrho+2)}\right)\max\{h^{4+2\varrho}, h^{2+2\varrho}\}$$
$$\le K_f^{(\varrho)}h^{2+2\varrho}, \tag{26}$$

where $K_f^{(\varrho)} = 3\left(\left(\frac{n^{2+\varrho}M}{\Gamma(\varrho+1)}\right)^2 + \frac{n}{2\Gamma^2(\varrho+2)}L_1(L^2+R^2)M^2 + \frac{L_2^2}{\Gamma^2(\varrho+2)}\right)$ is a constant independent of j and h.

Subsequently, for the second-term, we obtain

$$\begin{aligned}
\mathbb{E}[||\mathscr{E}_g(t_n)||^2] &:= \mathbb{E}\left[\left\| \frac{1}{\Gamma(\varrho)}\int_0^{t_n}(t_n-t)^{\varrho-1}g(t,u(t))d\omega(t)\right.\right.\\
&\quad\left.\left.-\frac{h^\varrho}{\Gamma(\varrho+2)}\left(g(t_n,u_{n-1})\eta(t_n)+\sum_{j=0}^{n-1}\sigma_{j,n}g(t_j,u_j)\eta(t_j)\right)\right\|^2\right],\\
&\le 3\mathbb{E}\left[\left\| \frac{1}{\Gamma(\varrho)}\int_0^{t_n}(t_n-t)^{\varrho-1}g(t,u(t))d\omega(t)-\frac{h^\varrho}{\Gamma(\varrho+2)}\sum_{j=0}^{n}\sigma_{j,n}g(t_j,u(t_j))\eta(t_j)\right\|^2\right]\\
&\quad+3\mathbb{E}\left[\left\| \frac{h^\varrho}{\Gamma(\varrho+2)}\sum_{j=0}^{n-1}\sigma_{j,n}(g(t_j,u(t_j))-g(t_j,u_j))\eta(t_j)\right\|^2\right]\\
&\quad+3\mathbb{E}\left[\left\| \frac{h^\varrho}{\Gamma(\varrho+2)}(g(t_n,u(t_n))-g(t_n,u_{n-1}))\eta(t_n)\right\|^2\right]\\
&\le \frac{3n^{2\varrho-1}M^2h^{2\varrho+3}}{4(2\varrho-1)\Gamma^2(\varrho)}\\
&\quad+\frac{3nh^{2\varrho}}{\Gamma^2(\varrho+2)}\sum_{j=0}^{n-1}\sigma_{j,n}^2\mathbb{E}\left[||\eta(t_j)||^2\right]\mathbb{E}\left[||(g(t_j,u(t_j))-g(t_j,u_j))||^2\right]\\
&\quad+\frac{3h^{2\varrho}}{\Gamma^2(\varrho+2)}\mathbb{E}\left[||\eta(t_n)||^2\right]\mathbb{E}[||(g(t_n,u(t_n))-g(t_n,u_{n-1}))||^2\Big].
\end{aligned}$$

Therefore, by means of the Lipschitz conditions, $\mathbb{E}\left[||\eta(t)||^2\right]=\frac{1}{h}$ and (25), after some simplications, we obtain

$$\begin{aligned}
\mathbb{E}\left[||\mathscr{E}_g(t_n)||^2\right] &\le \frac{3n^{2\varrho-1}M^2h^{2\varrho+3}}{4(2\varrho-1)\Gamma^2(\varrho)}+\frac{3\hat{L}^2h^{2\varrho+1}}{\Gamma^2(\varrho+2)}\left(n\sum_{j=0}^{n-1}\sigma_{j,n}^2+L_3^2\right)\\
&\le 3\left(\frac{n^{2\varrho-1}M^2}{4(2\varrho-1)\Gamma^2(\varrho)}+\frac{\hat{L}^2}{\Gamma^2(\varrho+2)}(nL_1+L_3^2)\right)\max\left\{h^{2\varrho+3},h^{2\varrho+1}\right\}.
\end{aligned}$$

Hence

$$\mathbb{E}\left[||\mathscr{E}_g(t_n)||^2\right]\le K_g^{(\varrho)}h^{2\varrho+1}, \tag{27}$$

where $K_g^{(\varrho)}=3(\frac{n^{2\varrho-1}M^2}{4(2\varrho-1)\Gamma^2(\varrho)}+\frac{\hat{L}^2}{\Gamma^2(\varrho+2)}(nL_1+L_3^2))$ is also another constant independent of j and h.

From (24), we have

$$||\mathscr{E}(t_n)||_{ms}^2\le 2K_f^{(\varrho)}h^{2\varrho+2}+2K_g^{(\varrho)}h^{2\varrho+1},$$

and

$$||\mathscr{E}(t_n)||_{ms}\le K^{(\varrho)}h^{\varrho+\frac{1}{2}}=\mathcal{O}(h^{\varrho+\frac{1}{2}}), \tag{28}$$

where $K^{(\varrho)}=(2K_f^{(\varrho)}+2K_g^{(\varrho)})^{\frac{1}{2}}$.

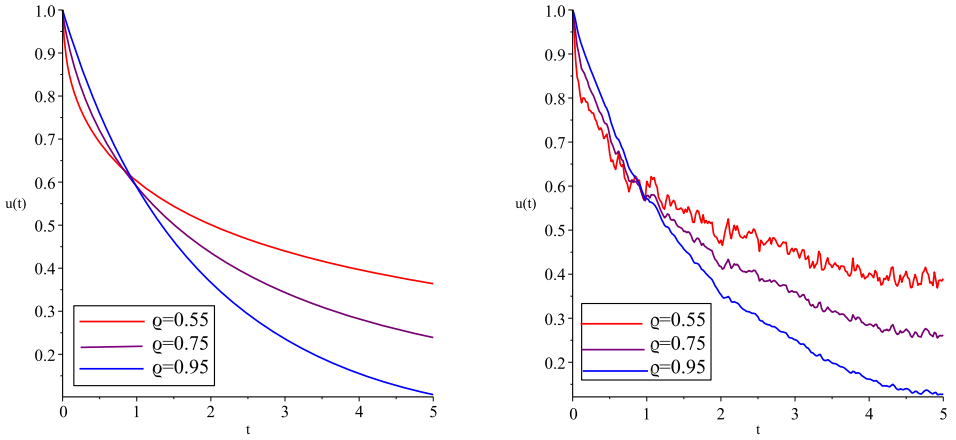

(a) FDDE–Langevin (b) FSDDE–Langevin

Figure 1. Numerical solutions of (31) with the proposed algorithm for $\delta = 0.1, \kappa = 0.5, \tau = 1, \varrho = \{0.55, 0.75, 0.95\}$, and step size $h = 0.02$.

5. Applications

In this section, the computational performance of the proposed method is analyzed in the perspective of the mean of the expected absolute error ($||\bar{\mathscr{E}}_N||_{ms}$) and the experimental convergence order (ECO) defined as

$$||\bar{\mathscr{E}}_N||_{ms} = \frac{1}{N}\sum_{k=1}^{N}\left(\mathbb{E}\left[||u_k^N - u_{2k}^{2N}||^2\right]\right)^{\frac{1}{2}}, \tag{29}$$

and

$$ECO = \log_2\left(\frac{||\bar{\mathscr{E}}_{2N}||_{ms}}{||\bar{\mathscr{E}}_N||_{ms}}\right), \tag{30}$$

where u_k^N and u_{2k}^{2N} are approximate values of $u(t_k)$, N represents the number of interior mesh points, and $h = \frac{T_f}{N}$ denotes the uniform step size. All the numerical experiments are calculated with the stats package under Maple v18 running in an Intel (R) Core (TM) i7-7500U CPU @ 2.70 GHz machine.

Model 5.1. *The fractional stochastic delayed dynamics in terms of a stationary probability density for the fractional stochastic delay Langevin differential equation can be stated as follows*

$$\begin{cases} {}_0^C\mathscr{D}_t^{\varrho}u(t) = -\kappa u(t-\delta) + \tau\dfrac{d\omega(t)}{dt}, & \dfrac{1}{2} < \varrho < 1, 0 < t < T_f, \\ u(t) = 1, & t \in [-\delta, 0] \end{cases} \tag{31}$$

where the parameters κ and τ are positive coefficients and δ is the delay time. The model (31) was studied in [52, 53] with $\varrho = 1$ for describing the statistical physics of vehicular traffic.

Figure 1 exhibits the stochastic effect on the fractional stochastic delay Langvin differential equation for $\delta = 0.1$, $\tau = 1$, $\kappa = 0.5$ with $\varrho = \{0.55, 0.75, 0.95\}$, and step size

Table 1. Model 1: Comparison of the $||\bar{\mathscr{E}}_N||_{ms}$, ECO, and CPU–time (sec) for $\varrho = \{0.55, 0.75, 0.95\}$, with $\delta = 0.1, \kappa = 0.5, \tau = 1$, and step sizes $h = \{0.02, 0.01, 0.005\}$ at $T_f = 5$.

ϱ	h	$\|\|\bar{\mathscr{E}}_N\|\|_{ms}$	ECO	$CPU-time(s)$
	0.02	1.4078×10^{-3}	1.678	4.228
0.55	0.01	2.0344×10^{-5}	2.345	16.287
	0.005	6.9554×10^{-6}	2.243	68.001
	0.02	1.9985×10^{-3}	1.589	4.228
0.75	0.01	7.8944×10^{-6}	2.551	16.193
	0.005	2.3130×10^{-6}	2.451	68.422
	0.02	2.7068×10^{-3}	1.511	4.181
0.95	0.01	2.3562×10^{-6}	2.814	16.115
	0.005	1.5370×10^{-6}	2.528	67.439

Table 2. Model 1: Approximation values of the mean, STD, 95% CI, first and third quartiles, skewness and kurtosis of the 50 simulated trajectories, with $\delta = 0.1, \kappa = 0.5, \tau = 1$, and $h = 0.02$ and $\varrho = \{0.55, 0.75, 0.95\}$, at $T_f = 5$.

Statistical indicators	0.55	0.75	0.95
Mean	0.363	0.238	0.105
Median	0.363	0.236	0.105
First quartile	0.348	0.227	0.094
Third quartile	0.373	0.246	0.113
Kurtosis	2.792	3.500	3.253
Skewness	0.485	0.696	0.611
STD	2.091×10^{-2}	1.829×10^{-2}	1.788×10^{-2}
95% CI	[0.322, 0.404]	[0.202, 0.274]	[0.070, 0.140]

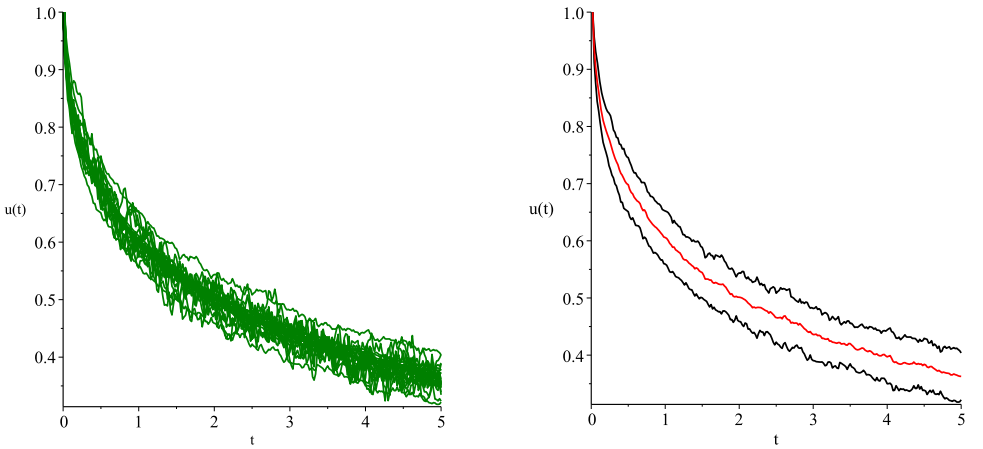

Figure 2. (Left) Numerical solution of (31) over 50 trajectories. (Right) The red line is the arithmetic mean of the process and the black lines illustrate 95% CI areas obtained with $\delta = 0.1, \kappa = 0.5$, $\tau = 1$, $\varrho = 0.55$, and step size $h = 0.02$ over the 50 trajectories of (31).

$h = 0.02$, in the interval $[0, 5]$. Table 1 presents the performance indices $||\bar{\mathscr{E}}_N||_{ms}$, ECO and CPU–time (sec) with several step sizes h for $\varrho = \{0.55, 0.75, 0.95\}$ in the interval $t \in [0, 5]$. Table 2 lists the approximation values of the mean, median, first and third quartiles, kurtosis, skewness, standard deviation (STD) and 95% CI of the 50 simulated trajectories with $\delta = 0.1$, for $\varrho = \{0.55, 0.75, 0.95\}$ at $T_f = 5$. Figure 2 (Left) depicts the numerical simulation results of 50 trajectories of the vehicular traffic dynamic for $u(t)$. In addition, the black lines in the right graph of Figure 2, represent the 95% CI area of the 50

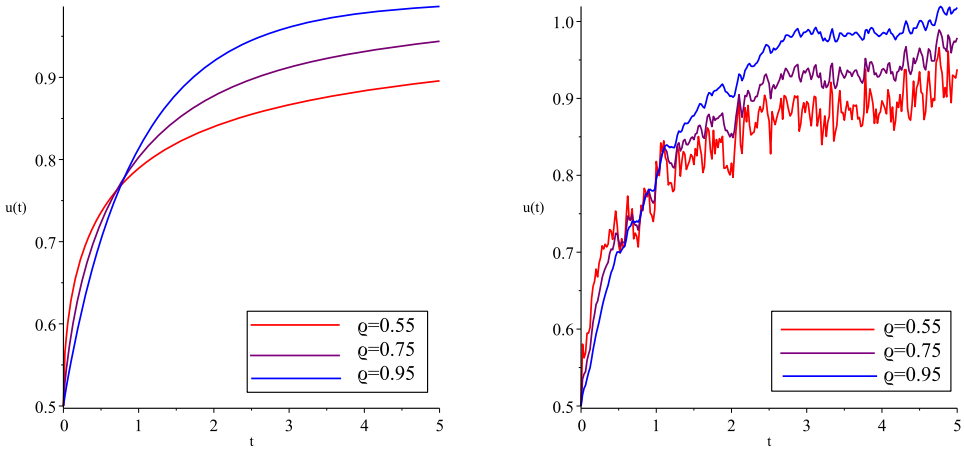

(a) FDDE–Mackey–Glass (b) FSDDE–Mackey–Glass

Figure 3. Numerical solutions of (32) with the proposed algorithm for $\kappa = 1$, $\lambda = 2$, $\delta = 5$, $\tau = 2$, $\varrho = \{0.55, 0.75, 0.95\}$, and step size $h = 0.02$.

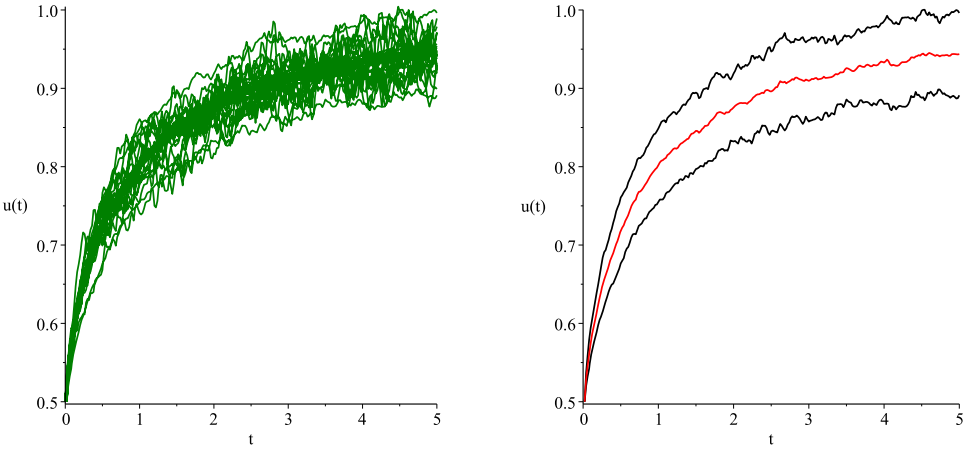

Figure 4. (Left) Numerical solution of (32) over 50 trajectories. (Right) The red line is the arithmetic mean of the process and the black lines illustrate 95% CI areas obtained with $\kappa = 1$, $\lambda = 2$, $\delta = 5$, $\tau = 2$, $\varrho = 0.75$, and step size $h = 0.02$ over the 50 trajectories of (32).

trajectories numerical solutions of the fractional stochastic delay Langevin differential equation. The red line represents the point-by-point sample mean of the trajectories.

Model 5.2. *Consider the fractional stochastic delay Mackey–Glass equation with a multiplicative noise input*

$$\begin{cases} {}_0^C\mathscr{D}_t^{\varrho} u(t) = \dfrac{\lambda u(t-\delta)}{1+u^{10}(t-\delta)} - \kappa u(t) + \tau u(t)\dfrac{d\omega(t)}{dt}, & \dfrac{1}{2} < \varrho < 1, 0 < t < T_f, \\ u(t) = 0.5, & t \in [-\delta, 0] \end{cases} \tag{32}$$

Table 3. Model 2: Comparison of the $||\bar{\mathscr{E}}_N||_{ms}$, ECO, and CPU–time (sec) for $\varrho = \{0.55, 0.75, 0.95\}$, with $\kappa = 1$, $\lambda = 2$, $\delta = 5$, $\tau = 2$, $T_f = 5$, and step sizes $h = \{0.02, 0.01, 0.005\}$.

ϱ	h	$\|\|\bar{\mathscr{E}}_N\|\|_{ms}$	ECO	$CPU-time(s)$
	0.02	1.7086×10^{-4}	2.217	4.649
0.55	0.01	5.6688×10^{-5}	2.123	17.581
	0.005	1.9059×10^{-5}	2.052	73.601
	0.02	8.6360×10^{-5}	2.392	4.446
0.75	0.01	2.5560×10^{-5}	2.295	17.503
	0.005	7.6148×10^{-6}	2.226	73.040
	0.02	4.5792×10^{-5}	2.554	4.477
0.95	0.01	1.1915×10^{-5}	2.462	17.643
	0.005	3.2668×10^{-6}	2.385	72.618

Table 4. Model 2: Approximation values of the mean, STD, 95% CI, first and third quartiles, skewness and kurtosis of the 50 simulated trajectories, with $\kappa = 1$, $\lambda = 2$, $\delta = 5$, $\tau = 2$, and $h = 0.02$ and $\varrho = \{0.55, 0.75, 0.95\}$, at $T_f = 5$.

Statistical indicators	0.55	0.75	0.95
Mean	0.898	0.944	0.985
Median	0.897	0.941	0.983
First quartile	0.875	0.923	0.971
Third quartile	0.919	0.954	0.998
Kurtosis	2.792	3.349	3.608
Skewness	0.532	0.758	0.768
STD	3.062×10^{-2}	2.682×10^{-2}	2.617×10^{-2}
95% CI	[0.838, 0.958]	[0.891, 0.996]	[0.934, 1.037]

where λ, κ, and τ are positive constants and δ is the delay time. The model (32) was analyzed in [54] with $\varrho = 1$ for describing the stochastic growth of density of blood cells.

Figure 3 depicts the numerical simulations of the fractional stochastic delay Mackey–Glass differential equation with different values of noise, $\tau = 0$ and $\tau = 2$, and fractional orders, $\varrho = \{0.55, 0.75, 0.95\}$, for $\kappa = 1$, $\lambda = 2$, $\delta = 5$, and $h = 0.02$. Figure 4 (Left) shows the simulation results of 50 trajectories of (32). In the right plot of Figure 4, the black lines represent the 95% CI area of the 50 trajectories numerical solutions of (32). The red line corresponds to the point-by-point sample mean of the trajectories. Table 3 gives the $||\bar{\mathscr{E}}_N||_{ms}$, ECO and CPU–time (sec) with several step sizes of h for $\varrho = \{0.55, 0.75, 0.95\}$, in the interval $t \in [0, 5]$. The numerical results reveal that for all values of ϱ the approximation errors decrease by reducing the step size, but the CPU–times increases as expected. Moreover, Table 4 shows the approximated values of the mean, median, first and third quartiles, kurtosis, skewness, standard deviation (STD), and 95% CI of the 50 simulated trajectories for several fractional orders at $T_f = 5$.

6. Conclusion

In this paper, an explicit technique for solving a class of fractional stochastic delay differential equations driven by Brownian motion was proposed. Under the Lipschitz condition and the properties of the Gaussian white noise, the convergence order of the algorithm was investigated. The new method allows the inclusion of stochasticity and delays in the dynamical models. The effects of stochasticity and delay were illustrated with the Langevin and Mackey-Glass models. Specifically, 95% confidence intervals of the Langevin and Mackey-Glass model's stochastic responses were effectively evaluated.

ORCID

B. P. Moghaddam http://orcid.org/0000-0003-4957-9028
A. Mendes Lopes http://orcid.org/0000-0001-7359-4370
J. A. Tenreiro Machado http://orcid.org/0000-0003-4274-4879
Z. S. Mostaghim http://orcid.org/0000-0003-2352-976X

References

[1] Henderson, D., Plaschko, P. (2006). *Stochastic Differential Equations in Science and Engineering*. World Scientific. DOI: 10.1142/5806.
[2] Singh, S., Ray, S. S. (2017). Numerical solutions of stochastic Fisher equation to study migration and population behavior in biological invasion. *Int. J. Biomath.* 10(07):1750103. DOI: 10.1142/S1793524517501030.
[3] Hattaf, K., Mahrouf, M., Adnani, J., Yousfi, N. (2018). Qualitative analysis of a stochastic epidemic model with specific functional response and temporary immunity. *Phys. A: Stat. Mech. Appl.* 490:591–600. DOI: 10.1016/j.physa.2017.08.043.
[4] Zmievskaya, G., Averina, T., Bondareva, A. (2015). Numerical solution of stochastic differential equations in the sense of stratonovich in an amorphization crystal lattice model. *Appl. Numer. Math.* 93:15–29. DOI: 10.1016/j.apnum.2014.05.006.
[5] Zmievskaya, G. I., Bondareva, A. L., Levchenko, T. V., Maino, G. (2015). Computational stochastic model of ions implantation. *AIP Conf. Proc.* 1648:230003.
[6] Gillard, N., Belin, E., Chapeau-Blondeau, F. (2017). Stochastic antiresonance in qubit phase estimation with quantum thermal noise. *Phys. Lett. A* 381(32):2621–2628. DOI: 10.1016/j.physleta.2017.06.009.
[7] Farhadi, A., Erjaee, G. H., Salehi, M. (2017). Derivation of a new Merton's optimal problem presented by fractional stochastic stock price and its applications. *Comput. Math. Appl.* 73(9):2066–2075. DOI: 10.1016/j.camwa.2017.02.031.
[8] in't Hout, K. J., Toivanen, J. (2018). ADI schemes for valuing European options under the Bates model. *Appl. Numer. Math.* 130:143–156. DOI: 10.1016/j.apnum.2018.04.003.
[9] Ballestra, L. V., Cecere, L. (2016). A fast numerical method to price American options under the Bates model. *Comput. Math. Appl.* 72(5):1305–1319. DOI: 10.1016/j.camwa.2016.06.041.
[10] Chen, X., Hu, P., Shum, S., Zhang, Y. (2016). Dynamic stochastic inventory management with reference price effects. *Oper. Res.* 64(6):1529–1536. DOI: 10.1287/opre.2016.1524.
[11] Einstein, A. (1905). On the motion of small particles suspended in liquids at rest required by the molecular–kinetic theory of heat. *Ann. Phys.* 17:549–560.
[12] von Smoluchowski, M. (1906). Zur kinetischen theorie der brownschen molekularbewegung und der suspensionen. *Ann. Phys.* 326(14):756–780. DOI: 10.1002/andp.19063261405.
[13] Langevin, P. (1908). Sur la théorie du mouvement brownien. *C. R. Acad. Sci. Paris* 146(530-533):530.
[14] Uhlenbeck, G. E., Ornstein, L. S. (1930). On the theory of the brownian motion. *Phys. Rev.* 36(5):823. DOI: 10.1103/PhysRev.36.823.
[15] Machado, J. A. T., Galhano, A. M., Lopes, A. M., Valério, D. (2016). *Solved Problems in Dynamical Systems and Control*. Institution of Engineering and Technology. DOI: 10.1049/pbce107e.
[16] Yaghoobi, S., Moghaddam, B. P., Ivaz, K. (2017). An efficient cubic spline approximation for variable-order fractional differential equations with time delay. *Nonlinear Dyn.* 87(2):815–826. DOI: 10.1007/s11071-016-3079-4.
[17] Biswas, K., Bohannan, G., Caponetto, R., Lopes, A. M., Machado, J. A. T. (2017). Introduction to fractional-order elements and devices. In: *Fractional-Order devices*. Springer International Publishing, pp. 1–20. DOI: 10.1007/978-3-319-54460-1_1.

[18] Moghaddam, B. P., Machado, J. A. T. (2017). A computational approach for the solution of a class of variable-order fractional integro-differential equations with weakly singular kernels. *Fract. Calc. Appl. Anal.* 20(4):1023–1042. DOI: 10.1515/fca-2017-0053.
[19] Dabiri, A., Butcher, E. A. (2017). Efficient modified Chebyshev differentiation matrices for fractional differential equations. *Commun. Nonlinear Sci. Numer. Simul.* 50:284–310. DOI: 10.1016/j.cnsns.2017.02.009.
[20] Dabiri, A., Butcher, E. A. (2017). Stable fractional Chebyshev differentiation matrix for the numerical solution of multi-order fractional differential equations. *Nonlinear Dyn.* 90(1): 185–201. DOI: 10.1007/s11071-017-3654-3.
[21] Chen, H., Lü, S., Chen, W. (2018). A unified numerical scheme for the multi-term time fractional diffusion and diffusion-wave equations with variable coefficients. *J. Comput. Appl. Math.* 330:380–397. DOI: 10.1016/j.cam.2017.09.011.
[22] Moghaddam, B. P., Aghili, A. (2012). A numerical method for solving linear non-homogenous fractional ordinary differential equation. *Appl. Math. Inf. Sci.* 6(3):441–445.
[23] Dabiri, A., Moghaddam, B. P., Machado, J. A. T. (2018). Optimal variable-order fractional PID controllers for dynamical systems. *J. Comput. Appl. Math.* 339:40–48. DOI: 10.1016/j.cam.2018.02.029.
[24] Machado, J. A. T., Moghaddam, B. P. (2018). A robust algorithm for nonlinear variable-order fractional control systems with delay, international journal of nonlinear sciences and numerical simulation. *Int. J. Nonlinear Sci. Numer. Simul.* 19(3-4):231–238. DOI: 10.1515/ijnsns-2016-0094.
[25] Bagley, R. L., Torvik, P. J. (1983). A theoretical basis for the application of fractional calculus to viscoelasticity. *J. Rheol.* 27(3):201–210. DOI: 10.1122/1.549724.
[26] Dabiri, A., Nazari, M., Butcher, E. A. (2016). The spectral parameter estimation method for parameter identification of linear fractional order systems. Presented at the American Control Conference (ACC), IEEE, Boston, MA, USA, July 6–8, Vol. 2016, pp. 2772–2777. DOI: 10.1109/acc.2016.7525338.
[27] Dabiri, A., Butcher, E. A., Nazari, M. (2017). Coefficient of restitution in fractional viscoelastic compliant impacts using fractional Chebyshev collocation. *J. Sound Vibr.* 388: 230–244. DOI: 10.1016/j.jsv.2016.10.013.
[28] Abdel-Rehim, E. (2009). From the Ehrenfest model to time-fractional stochastic processes. *J. Comput. Appl. Math.* 233(2):197–207. DOI: 10.1016/j.cam.2009.07.010.
[29] Chen, Z. Q., Kim, K. H., Kim, P. (2015). Fractional time stochastic partial differential equations. *Stoch. Process. Appl.* 125(4):1470–1499. DOI: 10.1016/j.spa.2014.11.005.
[30] Benchaabane, A., Sakthivel, R. (2017). Sobolev-type fractional stochastic differential equations with non-Lipschitz coefficients. *J. Comput. Appl. Math.* 312:65–73. DOI: 10.1016/j.cam.2015.12.020.
[31] Mirzaee, F., Samadyar, N. (2018). Using radial basis functions to solve two dimensional linear stochastic integral equations on non-rectangular domains. *Eng. Anal. Bound. Elem.* 92:180–195. DOI: 10.1016/j.enganabound.2017.12.017.
[32] Alejandre, M. P. A., Hernandez, F. J. A., Ortiz, J. S. (2016). Stochastic evolution equation with Riesz-fractional derivative and white noise on the half-line. *Appl. Numer. Math.* 104: 103–109. DOI: 10.1016/j.apnum.2015.05.002.
[33] Mirzaee, F., Samadyar, N. On the numerical solution of fractional stochastic integro-differential equations via meshless discrete collocation method based on radial basis functions. *Eng. Anal. Bound. Elem.* 100:246–255. DOI: 10.1016/j.enganabound.2018.05.006.
[34] Taheri, Z., Javadi, S., Babolian, E. (2017). Numerical solution of stochastic fractional integro-differential equation by the spectral collocation method. *J. Comput. Appl. Math.* 321: 336–347. DOI: 10.1016/j.cam.2017.02.027.
[35] Mostaghim, Z. S., Moghaddam, B. P., Haghgozar, H. S. (2018). Numerical simulation of fractional-order dynamical systems in noisy environments. *Comput. Appl. Math.* 37: 6433–6447. DOI: 10.1007/s40314-018-0698-z.

[36] Li, Q., Kang, T., Zhang, Q. (2018). Mean-square dissipative methods for stochastic age-dependent Capital system with fractional Brownian motion and jumps. *Appl. Math. Comput.* 339:81–92. DOI: 10.1016/j.amc.2018.07.018.

[37] Heydari, M., Mahmoudi, M., Shakiba, A., Avazzadeh, Z. (2018). Chebyshev cardinal wavelets and their application in solving nonlinear stochastic differential equations with fractional Brownian motion. *Commun. Nonlinear Sci. Numer. Simul.* 64:98–121. DOI: 10.1016/j.cnsns.2018.04.018.

[38] Mirzaee, F., Samadyar, N. (2018). Numerical solution of nonlinear stochastic Itô-Volterra integral equations driven by fractional Brownian motion. *Math. Methods Appl. Sci.* 41(4): 1410–1423. DOI: 10.1002/mma.4671.

[39] Mirzaee, F., Hamzeh, A. (2017). Stochastic operational matrix method for solving stochastic differential equation by a fractional Brownian motion. *Int. J. Appl. Comput. Math.* 3(S1):411–425. DOI: 10.1007/s40819-017-0362-0.

[40] Mirzaee, F., Samadyar, N., Hoseini, S. F. (2018). Euler polynomial solutions of nonlinear stochastic Itô–Volterra integral equations. *J. Comput. Appl. Math.* 330:574–585. DOI: 10.1016/j.cam.2017.09.005.

[41] Cui, J., Yan, L. (2011). Existence result for fractional neutral stochastic integro-differential equations with infinite delay. *J. Phys. A: Math. Theor.* 44(33):335201. DOI: 10.1088/1751-8113/44/33/335201.

[42] Kalamani, P., Baleanu, D., Selvarasu, S., Arjunan, M. M. (2016). On existence results for impulsive fractional neutral stochastic integro-differential equations with nonlocal and state-dependent delay conditions. *Adv. Differ. Equ.* 2016(1):163. DOI: 10.1186/s13662-016-0885-4.

[43] Muthukumar, P., Thiagu, K. (2016). Existence of solutions and approximate controllability of fractional nonlocal stochastic differential equations of order $1 < q < 2$ with infinite delay and Poisson jumps. *Differ. Equ. Dyn. Syst.* 23(2):213–235. DOI: 10.1007/s12591-016-0340-8.

[44] Bahuguna, D., Sakthivel, R., Chadha, A. (2017). Asymptotic stability of fractional impulsive neutral stochastic partial integro-differential equations with infinite delay. *Stoch. Anal. Appl.* 35(1):63–88. DOI: 10.1080/07362994.2016.1249285.

[45] Zhang, X., Agarwal, P., Liu, Z., Peng, H., You, F., Zhu, Y. (2017). Existence and uniqueness of solutions for stochastic differential equations of fractional-order $q > 1$ with finite delays. *Adv. Differ. Equ.* 2017(1):123. DOI: 10.1186/s13662-017-1169-3.

[46] Chatfield, C. (1983). *Statistics for Technology*. 3rd ed., London: Chapman and Hall. DOI: 10.1201/9780203738467.

[47] Banerjee, S. (2014). *Mathematical Modeling: Models, Analysis and Applications*. New York: CRC Press.

[48] Papoulis, A., Pillai, S. U. (2002). *Probability, Random Variables, and Stochastic Processes*. Tata McGraw-Hill Education.

[49] Øksendal, B. (2003). Stochastic differential equations. In: *Stochastic Differential Equations*. Berlin: Springer, pp. 65–84. DOI: 10.1007/978-3-642-14394-6-5.

[50] Samko, S. G., Kilbas, A. A., Marichev, O. I. (1993). *Fractional Integrals and Derivatives: Theory and Applications*. Philadelphia, USA: Gordon and Breach Science Publishers.

[51] Li, C., Chen, A., Ye, J. (2011). Numerical approaches to fractional calculus and fractional ordinary differential equation. *Comput. Phys.* 230(9):3352–3368. DOI: 10.1016/j.jcp.2011.01.030.

[52] Chowdhury, D. (2000). Statistical physics of vehicular traffic and some related systems. *Phys. Rep.* 329(4-6):199–329. DOI: 10.1016/S0370-1573(99)00117-9.

[53] Atay, F. M. (Ed.), (2010). *Complex Time-Delay Systems*. Berlin: Springer.

[54] Wang, X., Gan, S., Wang, D. θ- (2015). Maruyama methods for nonlinear stochastic differential delay equations. *Appl. Numer. Math.* 98:38–58. DOI: 10.1016/j.apnum.2015.08.004.